

# Beam energy and system dependence of rapidity-even dipolar flow

Niseem Magdy (For the STAR Collaboration)<sup>1\*</sup>

<sup>1</sup>Department of Chemistry, Stony Brook University, Stony Brook, NY, 11794-3400, USA

**Abstract.** New measurements of rapidity-even dipolar flow,  $v_1^{even}$ , are presented for several transverse momenta,  $p_T$ , and centrality intervals in Au+Au collisions at  $\sqrt{s_{NN}} = 200, 39$  and 19.6 GeV, U+U collisions at  $\sqrt{s_{NN}} = 193$  GeV, and Cu+Au, Cu+Cu, d+Au and p+Au collisions at  $\sqrt{s_{NN}} = 200$  GeV. The  $v_1^{even}$  shows characteristic dependencies on  $p_T$ , centrality, collision system and  $\sqrt{s_{NN}}$ , consistent with the expectation from a hydrodynamic-like expansion to the dipolar fluctuation in the initial state. These measurements could serve as constraints to distinguish between different initial-state models, and aid a more reliable extraction of the specific viscosity  $\eta/s$ .

## 1 Introduction

Heavy-ion collisions (HIC) at the Relativistic Heavy Ion Collider (RHIC) and the Large Hadron Collider (LHC) are aimed at studying the properties of the strongly interacting quark-gluon plasma (QGP) created in such collisions. Recent studies have emphasized the use of anisotropic flow measurements to study the transport properties of the QGP [1–7]. A crucial question in these studies was the role of initial-state fluctuations and their influence on the uncertainties associated with the extraction of  $\eta/s$  for the QGP produced in HIC [8, 9]. This work emphasizes new measurements for rapidity-even dipolar flow,  $v_1^{even}$ , which could aid a distinction between different initial-state models and facilitate the extraction of  $\eta/s$  with better constraints.

Anisotropic flow is characterized by the Fourier coefficients,  $v_n$ , obtained from a Fourier expansion of the azimuthal angle ( $\phi$ ) distribution of the emitted particles [10]:

$$\frac{dN}{d\phi} \propto 1 + 2 \sum_{n=1} v_n \cos(n(\phi - \Psi_n)), \quad (1)$$

where  $\Psi_n$  represents the  $n^{\text{th}}$ -order event plane, the coefficients  $v_1, v_2$  and  $v_3$  are called directed, elliptic and triangular flow, respectively. The flow coefficients  $v_n$  are related to the two-particle Fourier coefficients  $v_{n,n}$  as:

$$v_{n,n}(p_T^a, p_T^b) = v_n(p_T^a)v_n(p_T^b) + \delta_{NF}, \quad (2)$$

where  $p_T^a$  and  $p_T^b$  are the transverse momentum of particles (a) and (b), respectively, and  $\delta_{NF}$  is a so-called non-flow (NF) term, which includes possible contributions from resonance decays, Bose-Einstein correlations, jets, and global momentum conservation (GMC) [11–15]. The directed flow,  $v_1$ ,

---

\*e-mail: niseemm@gmail.com

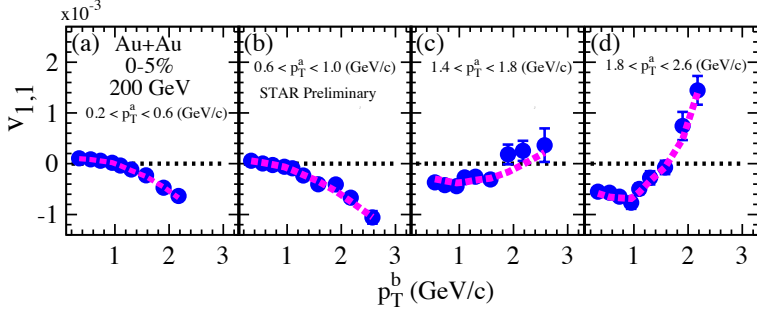


**Figure 1.**  $v_{1,1}$  vs.  $p_T^b$  for several selections of  $p_T^a$  for 0-5% central Au+Au collisions at  $\sqrt{s_{NN}} = 200$  GeV. The dashed curve shows the result of the simultaneous fit with Eq. 5.

can be separated into an odd function of pseudorapidity ( $\eta$ ) [16] which develops along the direction of the impact parameter, and a rapidity-even component [13, 17] which results from the effects of initial-state fluctuations acting in concert with a hydrodynamic-like expansion;  $v_1(\eta) = v_1^{even}(\eta) + v_1^{odd}(\eta)$ , where  $\Psi_1^{odd}$  and  $\Psi_1^{even}$  are uncorrelated. The magnitude of  $v_1^{even}$  is related to the fluctuations-driven dipole asymmetry  $\varepsilon_1$  and  $\eta/s$  [14, 17, 18].

## 2 Measurements

The correlation function technique was used to generate the two-particle  $\Delta\phi$  correlations:

$$C_r(\Delta\phi, \Delta\eta) = \frac{(dN/d\Delta\phi)_{same}}{(dN/d\Delta\phi)_{mixed}}, \quad (3)$$

where  $(dN/d\Delta\phi)_{same}$  represent the normalized azimuthal distribution of particle pairs from the same event and  $(dN/d\Delta\phi)_{mixed}$  represents the normalized azimuthal distribution for particle pairs in which each member is selected from a different event but with a similar classification for the vertex, centrality, etc. The pseudorapidity requirement  $|\Delta\eta| > 0.7$  was also imposed on track pairs to minimize possible non-flow contributions associated with the short-range correlations from resonance decays, Bose-Einstein correlations and jets.

The two-particle Fourier coefficients  $v_{n,n}$  are obtained from the correlation function as:

$$v_{n,n} = \frac{\sum_{\Delta\phi} C_r(\Delta\phi, \Delta\eta) \cos(n\Delta\phi)}{\sum_{\Delta\phi} C_r(\Delta\phi, \Delta\eta)}, \quad (4)$$

and then used to extract  $v_1^{even}$  via a simultaneous fit of  $v_{1,1}$  as a function of  $p_T^b$ , for several selections of  $p_T^a$  with Eq. 2:

$$v_{1,1}(p_T^a, p_T^b) = v_1^{even}(p_T^a) v_1^{even}(p_T^b) - C p_T^a p_T^b. \quad (5)$$

Here,  $C \propto 1/(\langle Mult \rangle \langle p_T^2 \rangle)$  takes into account the non-flow correlations induced by a global momentum conservation [14, 15] and  $\langle Mult \rangle$  is the mean multiplicity.

For a given centrality selection, the left hand side of Eq. 5 represents the  $N \times N$  matrix which we fit with the right hand side using  $N + 1$  parameters;  $N$  values of  $v_1^{even}(p_T)$  and one additional parameter  $C$ , accounting for momentum conservation [19]. Fig. 1 shows a representative result for this fitting procedure for 0 – 5% central Au+Au collisions at  $\sqrt{s_{NN}} = 200$  GeV. The dashed curve (obtained with Eq. 5) in each panel illustrates the effectiveness of the simultaneous fits, as well as the constraining power of the data. That is,  $v_{1,1}(p_T^b)$  evolves from negative to positive values as the selection range for  $p_T^a$  is increased.

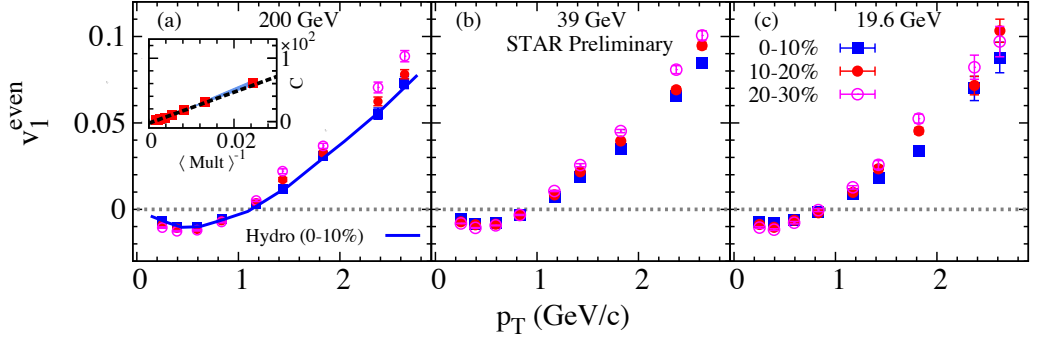


**Figure 2.** Extracted values of  $v_1^{even}$  vs.  $p_T$  for different centrality selections (0-10%, 10-20% and 20-30%) Au+Au collisions for several values of  $\sqrt{s_{NN}}$  as indicated; the  $v_1^{even}$  values are obtained via fits with Eq. (5). The solid line in panel (a) shows the result from a hydrodynamic calculations with  $\eta/s = 0.16$  [14]. The inset in panel (a) shows a representative set of the associated values of  $C$  vs.  $\langle Mult \rangle^{-1}$ .

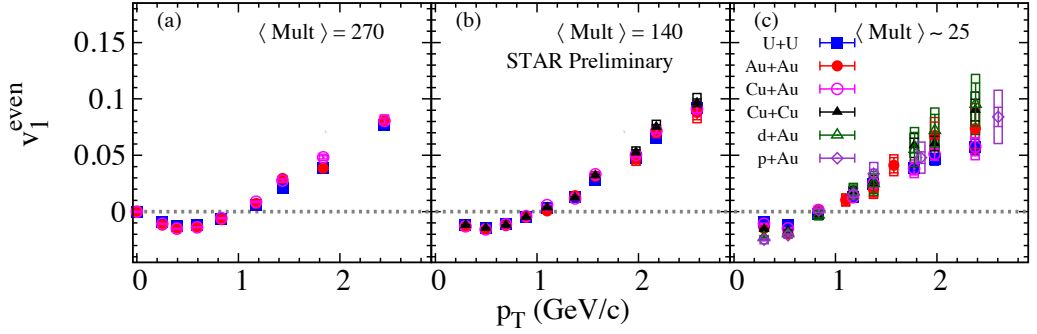


**Figure 3.** Extracted values of  $v_1^{even}$  vs.  $p_T$  for different  $\langle Mult \rangle$  selections for different collision system at  $\sqrt{s_{NN}} \sim 200$  GeV as indicated; the  $v_1^{even}$  values are obtained via fits with Eq. (5).

### 3 Results

Representative  $v_1^{even}$  results for Au+Au collisions at  $\sqrt{s_{NN}} = 200, 39,$  and  $19.6$  GeV and for different collision systems U+U at  $\sqrt{s_{NN}} = 193$  GeV, and Cu+Au, Cu+Cu, d+Au and p+Au at  $\sqrt{s_{NN}} = 200$  GeV are summarized in Figs. 2 and 3. The values of  $v_1^{even}(p_T)$  extracted for different centrality selections (0-10%, 10-20% and 20-30%) are shown in Fig. 2; the solid line in panel (a) shows the a hydrodynamic calculations with  $\eta/s = 0.16$ [14], which in good agreement with our measurements, the inset shows the corresponding results for the associated momentum conservation coefficient,  $C$ , extracted for several centralities at  $\sqrt{s_{NN}} = 200$  GeV. The  $v_1^{even}(p_T)$  values indicate the characteristic pattern of a change from negative  $v_1^{even}(p_T)$  at low  $p_T$  to positive  $v_1^{even}(p_T)$  for  $p_T > 1$  GeV/c, with a crossing point that shifts with  $\sqrt{s_{NN}}$ . They also indicate that  $v_1^{even}$  increase as the centrality become more peripheral, as might be expected from the centrality dependence of  $\varepsilon_1$ .

The extracted values of  $v_1^{even}(p_T)$ , for different collision systems are compared in Fig. 3 for different values of  $\langle Mult \rangle$ . Figs. 3(a), 3(b) and 3(c) indicate similar  $v_1^{even}(p_T)$  magnitudes for the systems specified at each  $\langle Mult \rangle$ , as well as the characteristic pattern of a change from negative  $v_1^{even}(p_T)$  at low  $p_T$  to positive  $v_1^{even}(p_T)$  for  $p_T > 1$  GeV. This pattern confirms the predicted trends for rapidity-even dipolar flow [13, 14, 17] and further indicates that for the selected values of  $\langle Mult \rangle$ ,  $v_1^{even}(p_T)$  does not show a strong dependence on the collision system. This apparent system independence of  $v_1^{even}(p_T)$  for the indicated  $\langle Mult \rangle$  values suggests that the fluctuations-driven initial-state eccentricity

$\varepsilon_1$ , is similar for the six collision systems. It also suggests that the viscous effects that are related to  $\eta/s$  are comparable for the matter created in each of these collision systems.

## 4 Conclusion

In summary, we have used the two-particle correlation method to carry out new differential measurements of rapidity-even dipolar flow,  $v_1^{even}$ , in Au+Au collisions at different beam energies, and in U+U, Cu+Au, Cu+Cu, d+Au and p+Au collisions at  $\sqrt{s_{NN}} \simeq 200$  GeV. The measurements confirm the characteristic patterns of an evolution from negative  $v_1^{even}(p_T)$  for  $p_T > 1$  GeV/c to positive  $v_1^{even}(p_T)$  for  $p_T > 1$  GeV/c, expected when initial-state geometric fluctuations act in concert with the hydrodynamic-like expansion to generate rapidity-even dipolar flow. This measurements provide additional constraints which are important to discern between different initial-state models, and to aid precision extraction of the temperature dependence of the specific shear viscosity.

## Acknowledgments

This research is supported by the US Department of Energy under contract DE-FG02-87ER40331.A008.

## References

- [1] D. Teaney, Phys.Rev. **C68**, 034913 (2003), nucl-th/0301099
- [2] R.A. Lacey, A. Taranenko, PoS **CFRNC2006**, 021 (2006), nucl-ex/0610029
- [3] B. Schenke, S. Jeon, C. Gale, Phys.Lett. **B702**, 59 (2011), 1102.0575
- [4] H. Song, S.A. Bass, U. Heinz, Phys.Rev. **C83**, 054912 (2011), 1103.2380
- [5] H. Niemi, G. Denicol, P. Huovinen, E. Molnar, D. Rischke, Phys.Rev. **C86**, 014909 (2012), 1203.2452
- [6] G.Y. Qin, H. Petersen, S.A. Bass, B. Muller, Phys.Rev. **C82**, 064903 (2010), 1009.1847
- [7] N. Magdy (STAR), J. Phys. Conf. Ser. **779**, 012060 (2017)
- [8] B. Alver, G. Roland, Phys. Rev. **C81**, 054905 (2010), [Erratum: Phys. Rev.C82,039903(2010)], 1003.0194
- [9] R.A. Lacey, D. Reynolds, A. Taranenko, N.N. Ajitanand, J.M. Alexander, F.H. Liu, Y. Gu, A. Mwai, J. Phys. **G43**, 10LT01 (2016), 1311.1728
- [10] A.M. Poskanzer, S.A. Voloshin, Phys. Rev. **C58**, 1671 (1998), nucl-ex/9805001
- [11] R.A. Lacey, Nucl. Phys. **A774**, 199 (2006), nucl-ex/0510029
- [12] N. Borghini, P.M. Dinh, J.Y. Ollitrault, Phys. Rev. **C62**, 034902 (2000), nucl-th/0004026
- [13] M. Luzum, J.Y. Ollitrault, Phys. Rev. Lett. **106**, 102301 (2011), 1011.6361
- [14] E. Retinskaya, M. Luzum, J.Y. Ollitrault, Phys. Rev. Lett. **108**, 252302 (2012), 1203.0931
- [15] G. Aad et al. (ATLAS), Phys. Rev. **C86**, 014907 (2012), 1203.3087
- [16] P. Danielewicz, R. Lacey, W.G. Lynch, Science **298**, 1592 (2002), nucl-th/0208016
- [17] D. Teaney, L. Yan, Phys. Rev. **C83**, 064904 (2011), 1010.1876
- [18] F.G. Gardim, F. Grassi, Y. Hama, M. Luzum, J.Y. Ollitrault, Phys. Rev. **C83**, 064901 (2011), 1103.4605
- [19] J. Jia, S.K. Radhakrishnan, S. Mohapatra, J. Phys. **G40**, 105108 (2013), 1203.3410